Available online at www.sciencedirect.com

SciVerse ScienceDirect

Ceramics International 39 (2013) 4281–4286

CERAMICS INTERNATIONAL

www.elsevier.com/locate/ceramint

# Effects of thermal oxidation on electromagnetic interference shielding properties of $SiC_f/SiC$ composites

Donghai Ding[a,*], Fa Luo[b], Wancheng Zhou[b]

[a]*College of Materials and Mineral Resources, Xi'an University of Architecture and Technology, Xi'an 710055, China*
[b]*State Key Laboratory of Solidification Processing, Northwestern Polytechnical University, Xi'an 710072, China*

Received 18 March 2012; received in revised form 29 October 2012; accepted 5 November 2012
Available online 10 November 2012

**Abstract**

$SiC_f/SiC$ composites containing PyC interphase were prepared by chemical vapor infiltration and their properties were investigated for electromagnetic interference (EMI) shielding applications in the frequency of 8.2–12.4 GHz. The room temperature direct current electrical conductivity ($\sigma_{dc}$) and EMI shielding effectiveness (SE) were tested after thermal oxidation for various time at 900 °C. It was found that the EMI was shielded mainly by absorption for both as-received and oxidized $SiC_f/SiC$ composites. Both $\sigma_{dc}$ and SE of $SiC_f/SiC$ composites decrease after thermal oxidation at 900 °C. It was proposed that the free carbon, including PyC interphase and free carbon in matrix and fibers, mainly determines the EMI SE of composites. The decrease of $\sigma_{dc}$ and SE of composites after oxidation are attributed to the consumption of free carbon. The SE of $SiC_f/SiC$ composites with a thickness of 2 mm remains above 15 dB after thermal oxidation for 4 h in air at 900 °C.


*Keywords:* $SiC_f/SiC$ composites; Electromagnetic interference shielding; Thermal oxidation

## 1. Introduction

Electromagnetic interference (EMI) has become a serious problem with the widespread use of electronic devices. Materials used for EMI shielding are attracting more and more attention for the purpose of protecting the workspace and the environment from the radiation emitted by electronic devices [1]. The common way of eliminating EMI is to use metal or carbon/polymer composites [1–7] as shielding packages. However, the high density and low corrosion resistance of metals limit their applications. In addition, carbon/polymer composites cannot be used as EMI shielding components working at high temperature. Ceramic matrix composites have their advantages to be used in oxidizing environment at high temperature. In the last few years, reports show that $Si_3N_4$–SiC and PyC–$Si_3N_4$ ceramics exhibit excellent EMI shielding properties [8,9]. And, Shi et al. prepared CNTs/zirconia composites by spark plasma sintering, and found that EMI shielding effectiveness of the composite increases with the increasing content of CNTs [10]. Wang et al. prepared ordered mesoporous carbon/fused silica composites by a controllable but simple sol–gel method followed by hot-pressing. The EMI shielding efficiency of ordered mesoporous carbon/fused silica composites is as high as 40 dB [11]. Furthermore, Yin et al. found that the EMI shielding effectiveness of yttria-stabilized zirconia/silicon carbide composites reach to 16.2 dB over the frequencies ranging from 8.2 GHz to 12.4 GHz [12].

It has been recognized that SiC fibers reinforced SiC matrix ($SiC_f/SiC$) composites are excellent thermal structural materials for aerospace, aeronautical and nuclear applications due to their outstanding high temperature strength, fracture toughness, chemical inertness and low activation characteristics [13,14]. It was found that there are obvious electric and dielectric losses in chemical vapor infiltration (CVI) SiC [9,15,16]. However, the reports on EMI shielding property of $SiC_f/SiC$ composites are rare. In the present paper, the $SiC_f/SiC$ composites were fabricated by CVI of PyC and SiC as interphase and matrix, respectively. The effects of thermal oxidation on EMI

*Corresponding author. Tel.: +86 29 82207830.
*E-mail address:* 290610692@qq.com (D. Ding).

0272-8842/$ - see front matter © 2012 Elsevier Ltd and Techna Group S.r.l. All rights reserved.
http://dx.doi.org/10.1016/j.ceramint.2012.11.007

shielding properties of $SiC_f/SiC$ composites were analyzed by testing its room temperature $\sigma_{dc}$ and scattering parameters.

## 2. Experimental

### 2.1. Materials fabrication

The KD-I SiC fibers were provided by National University of Defense Technology (China). Table 1 shows the parameters of SiC fibers [16]. The fabrics were braided by Nanjing Glass Fiber Institute (China). The fabrics structure is 2.5D shallow straight-joint shown in Fig. 1. The yarn densities of warp and weft are 6 and 8 yarn/cm, respectively. The total fiber volume fraction of the fabrics is about 40%.

The fabrication process of PyC interphase is according to that of Ding et al. [17]. Then, the SiC matrix was fabricated by CVI. The $SiCH_3Cl_3$ (MTS) is the gas precursor, and $H_2$ is used as carrier and diluent gases. The temperature and pressure of CVI process are 1100 °C and 5 kPa, respectively. And the flow ratio of $H_2$ as carrier gas and diluent gas are 300 and 30 ml/min, respectively. The infiltration time is 15 h.

### 2.2. Microstructure characterization

A Raman spectrometer (LabRAM HR800) was utilized using the 514.5 nm line of an argon-ion laser as the excitation source for spectroscopic characterization of SiC fibers, PyC interphase and CVI SiC matrix. The Raman test of fiber and matrix were carried out in composites. The PyC sample for Raman test was exploited from $Al_2O_3$ substrate. The microstructure of the composites was observed by a scanning electron microscope (SEM, S-4700, Hitachi, Japan).

Table 1
Parameters of KD-I SiC fibers.

| Fiber type | Diameter (μm) | Density (g/cm$^3$) | Tension strength (MPa) |
|---|---|---|---|
| KD-I | 14∼16 | 2.54 | 1800∼2200 |

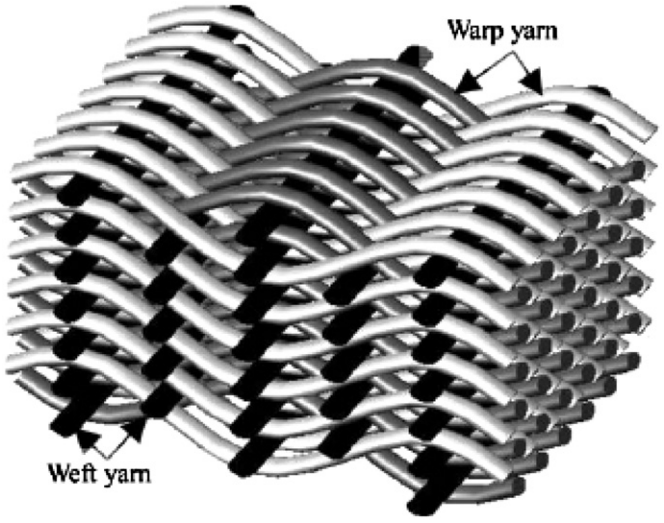


Fig. 1. Schematic showing of fabrics structure.

### 2.3. Measurement of scattering parameters and electrical conductivity

Based on previous literatures [8,9,12], the EMI SE of a material is defined as the ratio of transmitted powder ($P_t$) to incident powder ($P_i$) of an electromagnetic wave. The SE is measured in unit of dB and is given by

$$SE = -10\log\left(\frac{P_t}{P_i}\right) \quad (1)$$

The total EM shielding effectiveness ($SE_T$) of a material is the combination of the surface reflection ($SE_R$), the internal absorption ($SE_A$) and multiple internal reflection of the EM wave ($SE_M$). The combination is expressed as follows:

$$SE_T = SE_R + SE_A + SE_M \quad (2)$$

Generally, when $SE_T > 15$ dB, EMI is shielded mainly by reflection and/or absorption. Thus, EMI SE can be described by [12]

$$SE_T \approx SE_R + SE_A \quad (3)$$

The $SE_R$ and $SE_A$ can be calculated conveniently according to the reflection coefficient ($R$) and transmission coefficient ($T$) by the following equations:

$$SE_R = -10\log(1-R) \quad (4)$$

$$SE_A = -10\log(T/(1-R)) \quad (5)$$

where $R$ and $T$ can be directly calculated according to the following equations:

$$R = |S_{11}|^2 = |S_{22}|^2 \quad (6)$$

$$T = |S_{12}|^2 = |S_{21}|^2 \quad (7)$$

The scattering parameters (S-parameters: S11, S12, S22 and S21) in the frequency range 8.2–12.4 GHz were measured by a vector network analyzer (VNA; E8362B) using rectangular waveguide method. The size of test sample was 22.86 mm (length) × 10.16 mm (width) × 2 mm (thickness). The length and width directions were parallel to warp and weft directions, respectively.

The DC electrical conductivity ($\sigma_{dc}$) of composites was calculated according to

$$\sigma_{dc} = 1/\rho = \frac{L}{RS} \quad (8)$$

where $\rho$ is the special conductivity, $R$ is the resistance paralleled to weft of composites, $S$ is the cross section area of composites, and $L$ is the length of composites.

## 3. Results and discussion

### 3.1. Microstructure characterization

Fig. 2 shows the micrographs of cross section of as-prepared composites. As can be seen, there is a uniform PyC interphase between fiber and matrix, and its thickness is about 120 nm. The Raman spectrum of CVI SiC matrix, PyC interphase and KD-1 SiC fiber are shown in Fig. 3a, b and c, respectively. Observed from Fig. 3a–c, the D and G peaks at about 1350 and 1600 $cm^{-1}$ are attributed to $sp^3$ and $sp^2$ bonded carbon, respectively. It can be detected that both KD-I SiC fibers and CVI SiC matrix are rich in carbon. The rich carbon in CVI SiC matrix was attributed to different reaction kinetics of the silicon and carbon species decomposed from MTS. For CVI SiC matrix, the incompletely separated D and G peaks show that the graphitization degree of free carbon is lower than that of KD-1 fibers and PyC interphase. In addition, two peaks at 790 and 970 $cm^{-1}$ corresponding to β-SiC are obvious for CVI SiC matrix but not for KD-I SiC fibers. The reasons are proposed as follows: on one hand, the Raman scattering efficiency of carbon species can be assumed to be at least ten times higher than that of pure SiC materials due to their optical absorption [18]; on the other hand, the graphitization degree of free carbon is lower than that of KD-I fibers.

### 3.2. Changes of weight and DC electric conductivity

Table 2 shows the changes of room temperature conductivity and weight change after thermal oxidation at 900 °C. After thermal oxidation for 1 h, the conductivity decreases sharply from 0.112 to $1.32 \times 10^{-7}$ S/cm, then decreases slightly to $2.33 \times 10^{-8}$ after oxidation for 4 h. The weight decreases 3% after thermal oxidation for 1 h and increases slightly.

It was recognized that the oxidation of $SiC_f$/SiC composites with PyC interphase involves three phenomena [19,20]: (1) consumption of carbon according to Eqs. (9) and (10); (2) formation of silica according to Eqs. (11) and (12); (3) diffusion of oxygen and carbon oxides along the pores [18,19].

$$2C + O_2 = 2CO \quad (9)$$

$$C + O_2 = CO_2 \quad (10)$$

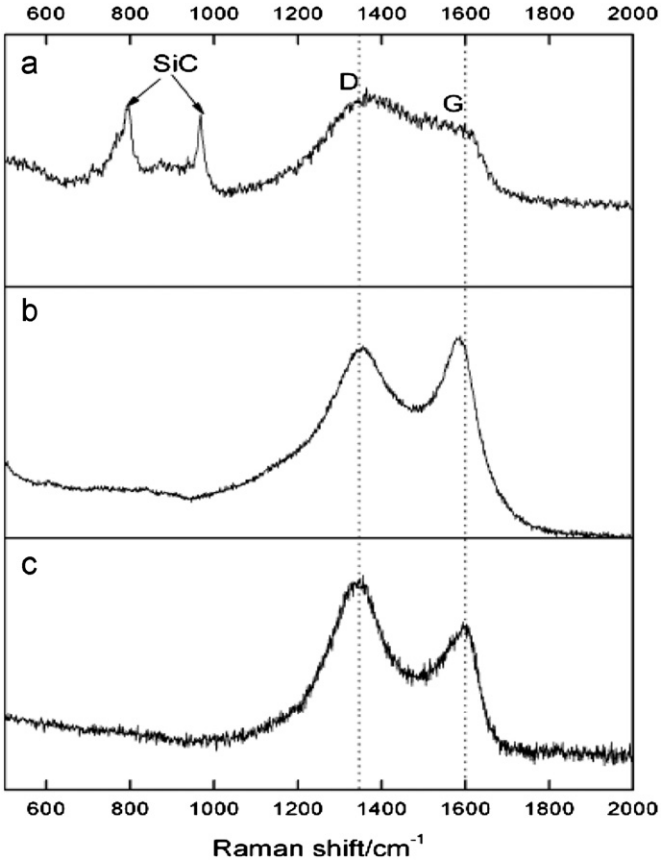


Fig. 3. Raman spectrum of CVI SiC matrix (a), PyC interphase (b) and KD-1 SiC fiber (c).

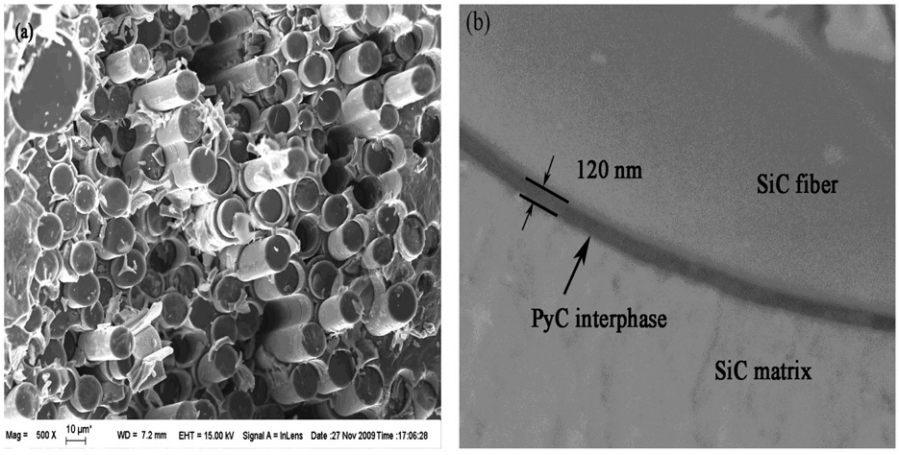


Fig. 2. SEM of low (a) and high (b) magnification fracture surface morphologies of $SiC_f$/SiC composites.

Table 2
Electrical conductivity and weight change of composites after thermal oxidation.

| Oxidation time (*h*) | As received | 1 h | 2 h | 3 h | 4 h |
|---|---|---|---|---|---|
| Electrical conductivity (S/cm) | 0.112 | $1.32\times10^{-7}$ | $1.18\times10^{-7}$ | $2.8\times10^{-8}$ | $2.33\times10^{-8}$ |
| Weight change (%) | – | −3.0 | −2.99 | −2.94 | −2.94 |

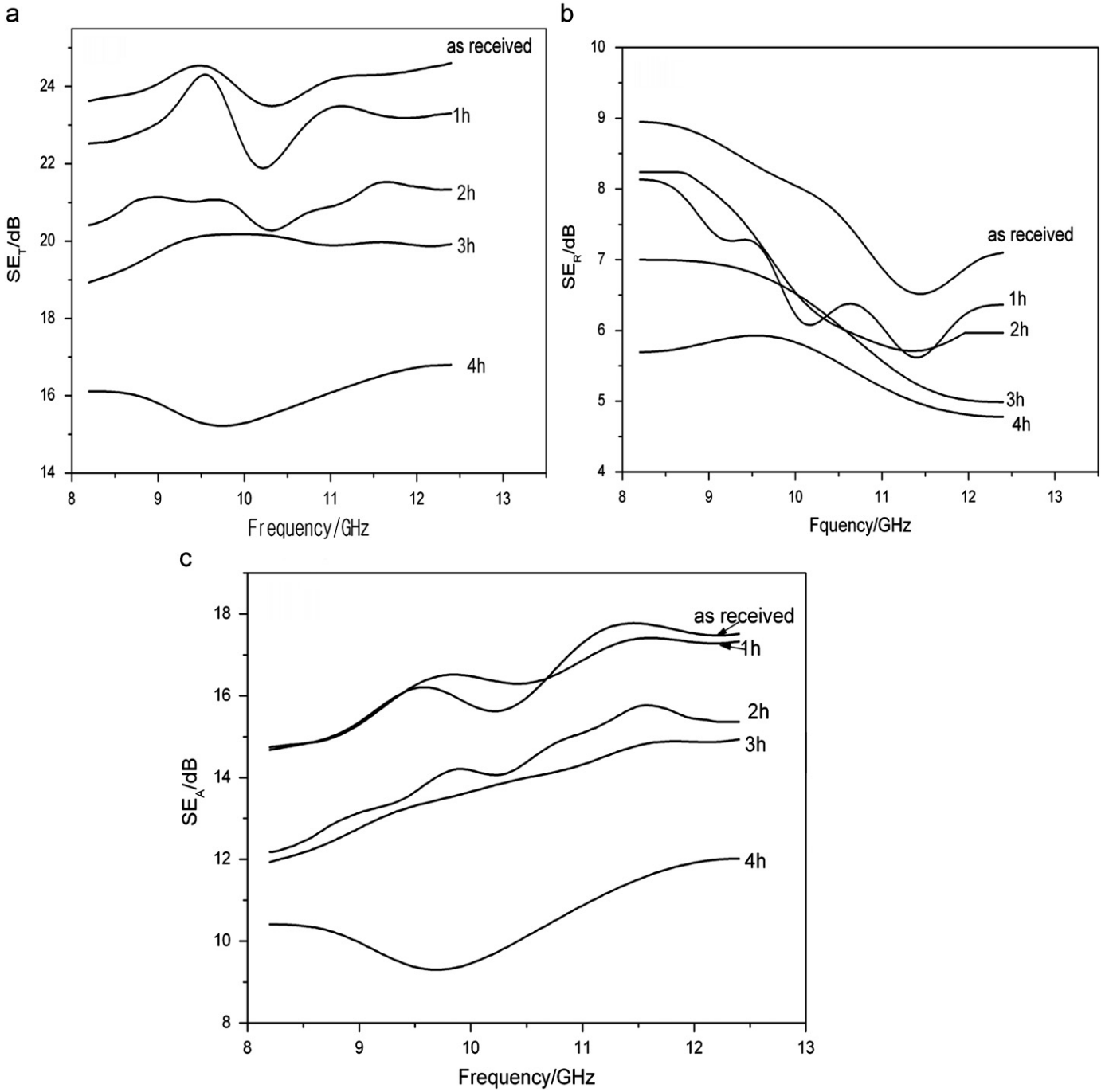


Fig. 4. $SE_R$, $SE_A$ and $SE_T$ of $SiC_f$/SiC composites after thermal oxidation for various times at 900 °C.

$$2SiC + 3O_2 = 2SiO_2 + 2CO \quad (11)$$

$$SiC + 2O_2 = 2SiO_2 + CO_2 \quad (12)$$

At higher temperature, the pores may be sealed by formation of silica and the oxidation of carbon is inhibited. Previous investigations show that the consumption of PyC interphase

and formation of silica can influence the mechanical properties of $SiC_f/SiC$ composites. However, in the present paper, we pay attention to the influences on electrical properties of $SiC_f/SiC$ composites.

The value of electrical conductivity of turbostratic carbon is much higher than pure SiC, so the conductivity of $SiC_f/SiC$ composites should mainly depend on turbostratic carbon in fibers, PyC interphase and SiC matrix. Thus, the consumption of turbostratic should be considered as the reason of weight loss and decreasing of conductivity of $SiC_f/SiC$ composites. In addition, the slight variations of weight and conductivity after 2 h thermal oxidation is due to the fact that turbostratic carbon is insulated with oxygen by silica.

### 3.3. EMI shielding properties $SiC_f/SiC$ composites

Fig. 4a–c shows the effects of thermal oxidation at 900 °C on $SE_R$, $SE_A$ and $SE_T$ of $SiC_f/SiC$ composites. It can be seen that EMI was shielded mainly by absorption in the case of $SiC_f/SiC$ composites, and the values of $SE_R$, $SE_A$ and $SE_T$ of composites decrease with increasing thermal oxidation time.

From the results above, it can be concluded that the EMI shielding properties of the composites deteriorate to some degree after thermal oxidation. The pure SiC materials cannot shield EMI because of its low electrical conductivity. Although the conductivity of turbostratic carbon is not available at present stage, the typical value of its conductivity is much higher than that of pure SiC materials. Generally, the relations between conductivity and EMI SE of composites are described as

$$SE_R = 39.5 + 10\log(\sigma/(2\pi f u)) \quad (13)$$

$$SE_A = 8.7d\sqrt{\pi f u \sigma} \quad (14)$$

where $f$ is the frequency of EM wave, $u$ is the magnetic permeability, $d$ is the specimen thickness, and $\sigma$ is the electrical conductivity [6]. For $SiC_f/SiC$ composites, the free carbon mainly determines the EMI SE of composites. Thus, the decrease in EMI SE should be attributed to the consumption of free carbon in $SiC_f/SiC$ composites. In addition, there are obvious distinctions between experimental data and theory data calculated according to Eqs. (12) and (13). The reason may be that Eqs. (12) and (13) are obtained for conductive materials [6].

Although the EMI shielding properties of $SiC_f/SiC$ composites deteriorate to some degree, the EMI SE remains above 15 dB after thermal oxidation at 900 °C for 4 h in air, indicating the advantages of $SiC_f/SiC$ composites as structural EMI shielding materials working in high temperature oxidizing environment.

## 4. Conclusions

The EMI shielding properties of $SiC_f/SiC$ composites containing PyC interphase were investigated. It was found that the absorption mainly contributes EMI shielding effectiveness of $SiC_f/SiC$ composites. And, the EMI SE of $SiC_f/SiC$ composites decreases obviously after thermal oxidation at 900 °C. It was proposed that the free carbon, including PyC and free carbon in matrix and fibers, mainly determines the EMI SE of composites. The deterioration of EMI shielding properties was attributed to the consumption of free carbon in the process of thermal oxidation. The EMI SE of $SiC_f/SiC$ composites with a thickness of 2 mm remains 15 dB above after thermal oxidation at 900 °C for 4 h in air, indicating the advantages of $SiC_f/SiC$ composites as structural EMI shielding materials working in high temperature oxidizing environment.

## Acknowledgments

This work was supported by the fund of the Scientific Research Program Funded by Shaanxi Provincial Education Department (12JK0598) and National Natural Science Foundation of China (Grant no. 51072165).

## References

[1] D.D.L. Chung, Electromagnetic interference shielding effectiveness of carbon materials, Carbon 39 (2001) 279–285.
[2] Y.S. Choi, Y.H. Yoo, J.G. Kim, S.K. Kim, A comparison of the corrosion resistance of Cu–Ni-stainless steel multilayers used for EMI shielding, Surface and Coatings Technology 201 (2006) 3775–3782.
[3] F.S. Hung, F.Y. Hung, C.M. Chiang, Crystallization and annealing effects of sputtered tin alloy films on electromagnetic interference shielding, Applied Surface Science 257 (2011) 3733–3738.
[4] E.G. Han, E.A. Kim, K.W. Oh, Electromagnetic interference shielding effectiveness of electroless Cu-plated PET fabrics, Synthetic Metals 123 (2001) 469–476.
[5] B. Fugetsu, E. Sano, M. Sunada, Y. Sambongi, T. Shibuva, T. Hiraki, Electrical conductivity and electromagnetic interference shielding efficiency of carbon nanotube/cellulose composite paper, Carbon 46 (2008) 1253–1269.
[6] M.H. Al-saleh, U. Sundararaj, Electromagnetic interference shielding mechanisms of CNT/polymer composites, Carbon 47 (2009) 1738–1746.
[7] Y. Huang, N. Li, Y.F. Ma, F. Du, F.F. Li, X.B. He, X. Lin, H.J. Gao, Y.S. Chen, The influence of single-walled carbon nanotube structure on the electromagnetic interference shielding efficiency of its epoxy composites, Carbon 45 (2007) 1614–1621.
[8] X.M. Li, L.T. Zhang, X.W. Yin, Synthesis and electromagnetic shielding property of pyrolytic carbon–silicon nitride ceramics with dense silicon nitride coating, Journal of the American Ceramic Society 95 (2011) 1038–1041.
[9] X.M. Li, L.T. Zhang, X.W. Yin, L.Y. Feng, Q. Li, Effect of chemical vapor infiltration of SiC on the mechanical and electromagnetic properties of $Si_3N_4$–SiC ceramic, Scripta Materialia 63 (2010) 657–660.
[10] S.L. Shi, J. Liang, The effect of multi-wall carbon nanotubes on electromagnetic interference shielding of ceramic composites, Nanotechnology 19 (2008) 255707.
[11] J.C. Wang, C.S. Xiang, Q. Liu, Y.B. Pan, J.K. Guo, Ordered mesoporous carbon/fused silica composites, Advanced Functional Materials 18 (2008) 2995–3002.
[12] X.W. Yin, Y.Y. Xue, L.T. Zhang, L.F. Cheng, Dielectric, electromagnetic absorption and interference shielding properties of porous yttria-stabilized zirconia/silicon carbide composites, Ceramics International 38 (2012) 2421–2427 2.5D.

[13] R. Naslain, Design, preparation and properties of non-oxide CMCs for application in engines and nuclear reactors: an overview, Composites Science and Technology 64 (2004) 155–170.
[14] K. Yoshida, Development of silicon carbide fiber-reinforced silicon carbide matrix composites with high performance based on interfacial and microstructure control, Journal of the Ceramic Society of Japan 118 (2010) 82–90.
[15] X.M. Yu, W.C. Zhou, F. Luo, W.J. Zheng, D.M. Zhu, Effect of fabrication atmosphere on dielectric properties of SiC/SiC composites, Journal of Alloys and Compounds 479 (2009) L1–L3.
[16] H.T. Liu, H.F. Cheng, J. Wang, G.P. Tang, Dielectric properties of the SiC fiber-reinforced SiC matrix composites with the CVD SiC interphases, Journal of Alloys and Compounds 491 (2010) 248–251.
[17] D.H. Ding, W.C. Zhou, F. Luo, D.M. Zhu, Influence of pyrolytic carbon coatings on complex permittivity and microwave absorbing properties of $Al_2O_3$ fiber woven fabrics, Transactions of Nonferrous Metals Society of China 22 (2012) 354–359.
[18] Y. Ma, S. Wang, Z.H. Chen, Raman spectroscopy studies of the high-temperature evolution of the free carbon phase in polycarbosilane derived SiC ceramics, Ceramics International 36 (2010) 2455–2459.
[19] R. Naslain, A. Guette, F. Rebillat, S. Le Gallet, F. Lamouroux, Oxidation mechanisms and kinetics of SiC-matrix composites and their constituents, Journal of Materials Science 39 (2004) 7303–7316.
[20] L. Filipuzzi, G. Camus, R. Naslain, Oxidation mechanisms and kinetics of 1D-SiC/C/SiC composites materials: I, an experimental approach, Journal of the American Ceramic Society 77 (1994) 459–4566 77.